



저작자표시-비영리-변경금지 2.0 대한민국

이용자는 아래의 조건을 따르는 경우에 한하여 자유롭게

- 이 저작물을 복제, 배포, 전송, 전시, 공연 및 방송할 수 있습니다.

다음과 같은 조건을 따라야 합니다:



저작자표시. 귀하는 원저작자를 표시하여야 합니다.



비영리. 귀하는 이 저작물을 영리 목적으로 이용할 수 없습니다.



변경금지. 귀하는 이 저작물을 개작, 변형 또는 가공할 수 없습니다.

- 귀하는, 이 저작물의 재이용이나 배포의 경우, 이 저작물에 적용된 이용허락조건을 명확하게 나타내어야 합니다.
- 저작권자로부터 별도의 허가를 받으면 이러한 조건들은 적용되지 않습니다.

저작권법에 따른 이용자의 권리는 위의 내용에 의하여 영향을 받지 않습니다.

이것은 [이용허락규약\(Legal Code\)](#)을 이해하기 쉽게 요약한 것입니다.

[Disclaimer](#)

치의과학박사 학위논문

Tubular Dentin Regeneration Using a CPNE7-Derived Functional Peptide

CPNE7 유래 기능성 펩타이드를 이용한
세관상아질의 재생

2021 년 2 월

서울대학교 대학원

치의과학과 세포 및 발생생물학 전공

이 윤 선

Tubular Dentin Regeneration Using a CPNE7-Derived Functional Peptide

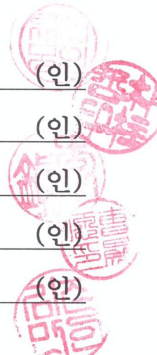
지도교수 박 주 철

이 논문을 치의과학박사 학위논문으로 제출함
2020 년 10 월

서울대학교 대학원
치의과학과 세포및발생생물학 전공
이 윤 선

이윤선의 치의과학박사 학위논문을 인준함
2020 년 10 월

위 원 장	류 현 모 (인)
부 위 원 장	박 주 철 (인)
위 원	이 진 (인)
위 원	조 성 원 (인)
위 원	김 진 만 (인)



Abstract

Tubular Dentin Regeneration Using a CPNE7-Derived Functional Peptide

Yoon Seon Lee

Department of Oral Histology-Development

Graduate School, Seoul National University

(Directed by Prof. **Joo-Cheol Park**, D.D.S., M.S.D., Ph.D.)

Regenerative dental medicine has rapidly progressed since the advancement of stem cell biology and material science. However, more emphasis has been placed on the success of regeneration than on how well the newly generated tissue retains the original organ structure and function.

Especially in tooth regeneration research, the compositional similarity of bone and dentin has undermined their distinction. Here, I developed a CPNE7 derivative synthetic oligopeptide (Cpne7-DP), which promotes odontoblast-like differentiation *in vitro* and tubular dentin formation *in vivo*. Moreover, I first show that CPNE7 and Cpne7-DP promote dentin regeneration in dentinal defects of various degrees and that the regenerated hard tissue demonstrates the characteristics of true dentin. Human dental pulp cells (HDPCs) and a mouse pre-odontoblast cell line, MDPC-23, were chosen for *in vitro* studies to characterize lineage-specific cell responses after Cpne7-DP treatment. Whether Cpne7-DP reproduces the dentin regenerative potential of CPNE7 was tested using a beagle dog model by generating dentinal defects of various degrees *in vivo*. Peritubular space occlusion was further examined by scanning electron microscopy and microleakage test, while overall mineralization capacity of Cpne7-DP was tested *ex vivo*. Comprehensive evaluation further validated its potential as a bioactive therapeutic agent.

The results suggest that the dual functions of Cpne7-DP in tubular dentin formation and peritubular space occlusion are promising for oral disease-targeted application, especially those involving dentinal loss and sensitivity.

Keywords : Odontoblasts, Dentinogenesis, Biomaterial(s), Mineralized tissue, Tissue Development

Student Number : 2014-23078

Contents

I. Introduction	1
II. Materials and Methods	3
III. Results	14
Table and Figures	22
IV. Discussion	45
V. Conclusions	49
VI. References	50
국문초록	54

I. Introduction

Loss of tooth dentin not only generates unpleasant sensitivity but ultimately leads to the weakening of whole tooth stability due to reduced dentin thickness. Among its varying causes, dental caries is the most prevalent chronic disease in both children and adults, affecting more than 5 billion people worldwide. Dental caries is caused by bacterial infection and resulting acidic byproducts that demineralize the tooth. Depending on the extent of the infection, the carious lesion either stops at the enamel or penetrates into the dentin (Pitts 2004). Exposed dentinal tubules in dental caries serve as a route for bacterial invasion that may result in various pulpal responses (Langeland 1987). In severe cases, tooth vitality is permanently lost (Nagaoka et al. 1995). A healthy tooth is composed of nearly 70% dentin enclosing the entire dental pulp, which is a pool of diverse stem cells (Gronthos et al. 2002). Accordingly, incessant efforts have been made to regenerate biologic dentin. However, most of the previously reported reparative tertiary dentin shows features of osteodentin, which is composed of bone-like structures with osteocyte-resembling cells entrapped in lacunae-like spaces (Kim 2017). The formation of osteodentin remains valuable because the damaged tissue is repaired with a newly mineralized barrier. Nonetheless, many reports highlight the significance of dentinal tubules in terms of defense mechanisms (Hahn and Best 2006; Maita et al. 1991; Pashley 1979). Moreover, the mineral density of osteodentin is less than that of physiologic tubular dentin (Hosoya et al. 2006). Therefore,

identification of biological materials capable of restoring dentin with tubular architecture is clinically important.

Based on the knowledge that epithelial-mesenchymal interaction is essential for tooth development, I previously discovered a dental epithelium-derived protein called Copine 7 (CPNE7). CPNE7 is an evolutionarily conserved, calcium-dependent phospholipid-binding protein and consists of two C2 domains in the N terminus and a von Willebrand factor A domain in the C terminus (Tomsig and Creutz 2002). Secreted from pre-ameloblasts, CPNE7 promotes odontoblast differentiation *in vitro* and induces dentin formation *ex vivo* (Lee et al. 2011; Oh et al. 2015; Park et al. 2019b). As a result, CPNE7 was suggested as a new molecule with the potential to diffuse across the dentin and induce tertiary dentinogenesis (Choung et al. 2016). The fact that recombinant CPNE7 is a cell-derived soluble bioactive molecule makes it a promising candidate for use in regenerative dental medicine.

As no peptide has yet been reported to form physiologic tubular dentin by stimulating odontoblasts or odontoblastic differentiation, I sought to design and synthesize a stable, cost-efficient, and manipulative functional peptide that mimics the functions of the protein CPNE7. Here, I thoroughly evaluate the tubular dentin forming capacity of CPNE7-derived oligopeptide (Cpne7-DP) and suggest their use as future therapeutic agents for dental defects such as dental caries.

II. Materials and Methods

Tooth Defect Models with Canine Teeth

For in vivo canine studies, a total of 10 beagle dogs (2 y) were operated on, with all of them reaching end points. For each animal, 4 to 6 maxillary premolars and 6 mandibular premolars were used, depending on their periodontal conditions. Control and experimental groups were allocated to each and every animal so that possible biases resulting from individual nutritional, behavioral, and pulpal conditions could be eliminated. Compared to small animal studies, the sample size was necessarily limited for feasibility and ethical reasons. While the exact numbers for each experiment are included in the figure legends, at least 6 premolars and up to 12 premolars were assigned to every control and experimental group. Investigators performing beagle operation and sampling were not blinded, while investigators involved in histological analysis were blinded. All experiments using animals followed protocols approved by the Institutional Animal Care and Use Committee of Seoul National University (SNU-180416-2-1 and SNU-171020-5-2).

Beagle dogs of 1–2 years of age were used for three independent experiments. After disinfecting the cervical regions of the maxillary and mandibular premolars with 0.5% chlorhexidine, dish-shaped class V cavities were prepared using a #4 high-speed round bur (head diameter, 1.4 mm). For shallow cavities, the drilling stopped when half to two-thirds of the bur head penetrated the tooth structure, depending on the tooth size. For deep

cavities, the drilling stopped when the color of the remaining dentin looked reddish gray. The smear layer was removed with a gentle application of 17% EDTA. After sufficient irrigation, surgical sites were dried with a cotton pellet. For CPNE7 function analysis, the cavities were either untreated or treated with a topical application of rCPNE7 (recombinant CPNE7) protein (1 µg total rCPNE7 per tooth in a buffer containing 25 mM Tris-HCl, 100 mM glycine, and 10% glycerol). After a brief incubation for diffusion, the cavities were then filled with either glass ionomer (GI) cement (GC; Fuji II LC; GC America Inc., Alsip, IL, USA), composite resin (Filtek Supreme Ultra Flowable Restorative; 3 M, MN, USA) or intermediate restorative material (IRM; Dentsply Sirona, York, PA, USA). For peptide function analysis, an HIV-1 Tat-derived cell-penetrating peptide was used as control. In addition to the abovementioned shallow and deep cavity models, complete pulp exposure was performed for peptide analysis. For complete pulp exposure, the drilling stopped when a pin-point exposure of the pulp was generated and bleeding was evident. Cotton pellets soaked in saline were used for bleeding control. Cavities with exposed pulps were divided into two groups for the experiment. Group 1 received only GI cement filling, group 2 received GI cement filling after MTA (ProRoot MTA; Dentsply Sirona, York, PA, USA) sealing, and group 3 received GI cement filling after MTA mixed with CPNE7-derived oligopeptide (Cpne7-DP) sealing.

The premolar areas were dissected 3, 6, or 12 weeks following surgery, and samples were immersed in 4% paraformaldehyde and kept for an additional 24 h at 4 °C. Decalcification was performed in 10% formic acid,

and the specimens were then embedded in paraffin. Serial 5- μ m-thick sections were H&E stained.

TUNEL Assay

Apoptotic cells were detected using the TUNEL kit (Roche Biochemicals, Basel, Switzerland), according to the manufacturer's instructions. Endogenous peroxidase activity within the tissue sections were blocked in 3% H₂O₂ prior to enzymatic labeling. To yield a colored reaction product, enzymatically labeled cells were then incubated with 3,3-diaminobenzidine tetrahydrochloride. Visualization was achieved by incubating the sections with diaminobenzidine tetrahydrochloride (DAB), and subsequent counter-staining with hematoxylin. Positive TUNEL signals were converted to red color using IHC Profiler of Image J software (National Institute of Health, USA).

Cell Culture

MDPC-23 cells were provided by Dr. J.E. Nor (University of Michigan, Ann Arbor, MI, USA) and cultured in Dulbecco's modified Eagle medium (DMEM; Gibco BRL., Carlsbad, CA, USA). C3H10T1/2 cells were obtained from the American Type Culture Collection (ATCC, Manassas, VA, USA) and cultured in RPMI 1640 medium (Gibco BRL). Both cell lines were supplemented with 10% heat-inactivated fetal bovine serum (FBS; Gibco BRL) and antibiotic-antimycotic reagents (Gibco BRL) at 37°C in a 5% CO₂ atmosphere. Impacted human third molars from patients between the ages of 18 and 22 were provided by the Seoul National University Dental Hospital.

The experimental protocol was approved by the Institutional Review Board (IRB No:S-D20140007). Informed consent was obtained from every patient. Isolation of whole pulp cells was performed as previously described [11], and cells were cultured in minimum essential media α (MEM- α ; Gibco BRL) for use in in vitro and ex vivo experiments. For human dental pulp cells (hDPCs) and MDPC-23 cell differentiation, 80–90% confluent cells were cultured in corresponding media supplemented with 5% FBS, ascorbic acid (50 $\mu\text{g}/\text{mL}$), and β -glycerophosphate (10 mM) for up to 3 weeks. Passages from 2 to 4 were used for hDPSCs, and 23 to 25 were used for MDPC-23 cells.

Peptide Synthesis

Cpne7-DP consists of a synthetic peptide corresponding to the 10 amino acid residue 344–353 fragment (KYKQKRRSYK) of the hCPNE7 protein. The peptides were synthesized using the Fmoc (9-fluorenylmethoxycarbonyl)-based solid-phase method and characterized by Lugen Sci. Co., Ltd. (Bucheon, Korea). The purity of the peptides used in this study was greater than 97%, as determined by high-performance liquid chromatography.

Luciferase Assay

MDPC-23 cells were seeded on a 24-well plate at a density of 5×10^4 cells/wells and transfected with Lipofectamine PlusTM reagent (Invitrogen, Carlsbad, CA, USA) after 24 h. For each transfection, 0.4 μg luciferase reporter plasmid pGL3 basic (Control) and pGL3LUC dspp (-750 ~ +61)

were used. Transfected cells were treated with Cpne7-DP or recombinant CPNE7 protein for 48 h and were then lysed for luciferase activity assessment using the luciferase reporter gene assay system (Roche Applied Science, Indianapolis, IN, USA) according to the manufacturer's instructions. The measurements were performed with a luminometer (FLUOStar OPTIMA, BMC Laboratory, Offenburg, Germany). Three independent experiments with triplicate samples were analyzed.

Cytotoxicity Assessment

To evaluate the effects of Cpne7-DP on hDPCs proliferation, an MTT [3-(4,5-Dimethyl thiazol-2-yl)-2,5-diphenyl tetrazolium bromide, a tetrazole] assay (Sigma-Aldrich, Saint Louis, MO, USA) was performed. Cells were seeded on a 96-well plate at a density of 3×10^3 cells/well and treated with Cpne7-DP after 24 h. Cells were cultured for upto 5 days, and MTT analyses were performed on days 0, 1, 3, and 5. After washing with phosphate-buffered saline (PBS), 20 mL of MTT was added to each well and incubated for 4 h at 37°C. After removing the MTT solution, the converted dye was dissolved in Me₂SO and measured by reading the absorbance at a wavelength of 540 nm with a microplate reader (Multiskan EX; Thermo Electron Corp., Waltham, MA, USA). Three independent experiments with triplicate samples were analyzed.

Real-time Polymerase Chain Reaction Analysis

Total RNA was extracted from cells with TRIzol reagent according to the manufacturer's instructions (Invitrogen, Carlsbad, CA, USA). Three μ g

of RNA was reverse transcribed using Superscript III reverse transcriptase (Invitrogen) and oligo (dT) primers (Invitrogen). One mL of cDNA was subjected to PCR amplification using the ABI PRISM 7500 sequence detection system (Applied Biosystems, Carlsbad, CA, USA) using SYBR Green PCR Master Mix (Applied Biosystems) according to the manufacturer's instructions. PCR was performed using the following conditions: 94°C for 1 min, 95°C for 15 s, and 60°C for 34 s, for 40 cycles. All reactions were performed in triplicate and normalized to reactions using the housekeeping gene glyceraldehyde 3-phosphate dehydrogenase (GAPDH). Relative changes in gene expression were calculated using the comparative threshold cycle (CT) method. The sequences of the real-time PCR primers used in the study are listed in Table 1.

Western blot analysis

Whole cell lysates were harvested in a lysis buffer consisting of 50 mM Tris-HCl, pH 7.4, 150 mM NaCl, 1% Nonidet P-40, 1 mM EDTA, and 1 mM PMSF supplemented with protease inhibitors (Roche Molecular Biochemicals, Mannheim, Germany). The supernatant after centrifugation at 13,000 x g for 30 min was collected for analysis. DCTM protein assay system (Bio-Rad Laboratories, Hercules, CA, USA) was used to measure protein concentrations. Twenty five μ g of proteins were resolved using 10% polyacrylamide gel electrophoresis and transferred to a PVDF membrane, which was then blocked with PBST (10 mM phosphate-buffered saline, pH 7.0, and 0.1% Tween-20) buffer containing 5% non-fat dry milk for 1 h at room temperature. After washing, the blots were incubated with primary

antibodies indicated in Table 2, overnight at 4°C with gentle shaking. Before incubation with anti-rabbit or anti-mouse immunoglobulin G conjugated to horseradish peroxidase in PBST for 1 h at room temperature, blots were washed 3 times for 10 min in PBST. Labeled protein bands were detected under an enhanced chemi-luminescence reagent (ECL; Santa Cruz Biotechnology, Dallas, TX, USA) according to the manufacturer's guidelines. Semi-quantitative analyses were performed using Image J software (National Institute of Health).

Ex Vivo Transplantation and Histological Analysis

Human root segments (<5 mm in thickness) were prepared from extracted human teeth after pulp tissues were removed according to the previously reported protocol (Choung et al. 2013). Human DPCs (2×10^6) were mixed with hydroxyapatite/tricalciumphosphate (HA/TCP) ceramic powder (Zimmer, Warsaw, IN, USA) alone or with Cpne7-DP (10 μ g) in an 0.5% fibrin gel and then transplanted subcutaneously into immunocompromised mice (NIH-bg-nu-xid; Harlan Laboratories, Indianapolis, IN, USA) for 6 or 12 weeks. Dentin/pulp-like tissue formation in the emptied root canal space was evaluated after mixing hDPCs (2×10^6) with Cpne7-DP (10 μ g) in a 0.5% fibrin gel and inserting the mixture into emptied root canal space of the human root segments for 6 weeks. Harvested samples were fixed in 4% paraformaldehyde, decalcified in 10% EDTA (pH 7.4), embedded in paraffin, and stained with hematoxylin and eosin (H&E) (Vector Laboratory, Burlingame, CA, USA), Masson's Trichrome Stain (Polysciences, Warrington, PA, USA), or processed for immunohistochemical analysis. For

immunohistochemistry, the sections were incubated overnight at 4°C with rabbit polyclonal DSP and BSP produced, as described previously (Lee et al. 2009) at a dilution of 1:150. Biotin-labeled goat anti-rabbit IgG (Vector Laboratory) was incubated with the sections at room temperature for 30 min, which were then reacted with the avidin-biotin-peroxidase complex (Vector Laboratory). Signals were converted using a diaminobenzidine kit (Vector Laboratory). Nuclei were stained with hematoxylin.

Immunofluorescence Staining

For peptide translocation and localization analysis, a Cy5 Fast Conjugation Kit (ab188288, Abcam, Cambridge, MA, USA) was used to tag Cpne7-DP according to the manufacturer's instructions. MDPC-23 cells were treated with Cy5-labeled Cpne7-DP (10 µg/mL) and fixed 3 h later. Before fixing with 4% paraformaldehyde in PBS, cells in Laboratory-Tek chamber slides (Nunc, Rochester, NY, USA) were washed with PBS. Cells were then visualized using fluorescence microscopy (AX70, Olympus, Tokyo, Japan). DAPI (Sigma-Aldrich) was used to identify the chromosomal DNA in the nucleus (1:1000 dilution). Reagents used are listed in Table 3.

Transient Transfection

C3H10T1/2 cells or hDPCs were seeded on 60 mm culture plates at a density of 1×10^6 cells. The cells were transiently transfected with DDK(Flag)-tagged CPNE7 using the Metafectene Proreagent (Biontex Laboratories GmbH, Munich, Germany) according to the manufacturer's instructions.

Scanning Electron Microscopic Analysis

Samples were fixed in 0.1 M cacodylate buffer (pH 7.3) containing 2.5% glutaraldehyde for 30min and in 0.1 M cacodylate buffer (pH 7.4) containing 1% osmium tetroxide for 1h. Samples were then rapidly dehydrated through an ethanol gradient. After sputter coating with gold, samples were observed under a scanning electron microscope (S-4700, HITACHI, Tokyo, Japan).

Specimen Preparation

Human third molars were collected at the Seoul National University Dental Hospital (Seoul, Korea), and the experimental protocol was approved by the Institutional Review Board (IRB No: S-D20140007). Teeth were decoronated to 2–3 mm using a safe diamond disc (Isomet, Buehler Ltd., Düsseldorf, Germany) to eliminate the coronal enamel layer and expose the dentin surface. Teeth were then treated with 5 mL of 32% phosphoric acid solution for 5 min to completely open the dentinal tubules. To remove the residual smear layer, specimens were ultrasonicated in deionized water twice for 5 min each and then rinsed with PBS three times.

CLSM Specimen Preparation and Analyses

Cpne7-DP was tagged with Rhodamin B dye using the Rhodamine Fast Conjugation kit (ab188286, Abcam, Cambridge, MA, USA) according to the manufacturer's instructions. Rhodamin B-labeled Cpne7-DP (20 µg) was applied to the dentin surfaces of specimens with the help of disposable microbrushes for 1min, and then specimens were washed with PBS three

times. Subsequently, the specimens were longitudinally sectioned at a thickness of 0.5 mm using a safe diamond disc. The sections were mounted onto glass slides and scanned under a confocal laser scanning microscope (LSM 700; Carl Zeiss, Jena, Germany).

Alizarin Red S Staining

MDPC-23 cells were seeded on 60 mm culture plates at a density of 1×10^6 cells and cultured in differentiation medium for 14 days with or without Cpne7-DP. The formation of mineralized nodules was evaluated by staining with alizarin red S (Sigma-Aldrich) solution in 0.1% NH_4OH at pH 4.2 for 20 min at room temperature.

Microleakage Test

The extent of tubule occlusion was measured with the previously reported nano-fluid movement measuring device (Park et al. 2019a). Apical 3 mm of extracted beagle incisors was cut with a high-speed diamond bur (TF-13, MANI, Tokyo, Japan) to expose the root canals. A 0.9 mm metal tube was inserted, while 32% phosphoric acid, adhesive agent (Singlebond Universal, 3M ESPE, St Paul, MN, USA) and flowable composite resin (Filtek Supreme Ultra Flowable Restorative; 3M, Alexandria, MN, USA) were applied to bond with the metal tube. All areas except for the defect region were covered with nail varnish several times. The prepared specimens were kept in distilled water. A nano-fluid movement measuring device (NanoFlow, IB Systems, Seoul, Korea) recognizes the movement of bubbles due to leakage when distilled water is left to flow from the tooth apex to the exposed

dentin at 70 cm H₂O. All measurements were taken 40 min after the specimens were connected, while the first 20 min of outflow was excluded.

Statistical Analysis

All data were expressed as the mean \pm standard deviation of triplicate experiments. Statistical significance was analyzed using a non-parametric Mann–Whitney U test for comparisons between two groups, and one-way analysis of variance (ANOVA) with Bonferroni correction for comparisons between more than two groups by the SPSS software version 25. P values less than 0.05 were considered statistically significant.

III. Results

Treatment of Recombinant CPNE7 Promotes the Regeneration of Tubular Dentin in Shallow and Deep Cavity Models

To assess the effects of recombinant CPNE7 (rCPNE7) in varying extents of dentinal defects, both shallow and deep cavities were artificially generated in beagle dog premolars (Figure 1) and divided into two groups each (n = 6 for all groups): glass ionomer (GI), cement filling only (Control), and GI cement filling after topical application of rCPNE7. After three weeks, in the shallow cavity models where the underlying odontoblasts were expected to be mildly deterred, no new hard tissue formation was detected in the pulp cavity of the control group. In contrast, newly generated tertiary dentin retaining the physiologic tubule structure was observed beneath the defect in the rCPNE7-treated group (Figure 2A). In the deep cavity models where the underlying odontoblasts were expected to be severely damaged, no evidence of dentin repair was found in the control group. Moreover, the odontoblasts beneath the cavity became more rounded than the adjacent odontoblasts underlying the non-cavity areas, indicating morphological distortion. In the rCPNE7-treated deep cavity, however, newly generated tertiary dentin was present beneath the remaining dentin at the cavity-preparation sites with regular cell alignment (Figure 2B). Terminal deoxynucleotidyl transferase dUTP nick end labeling (TUNEL) demonstrated significantly reduced cell death under the newly generated dentin in the rCPNE7-treated group (Figure 3). When the samples were collected six weeks after the experiment instead

of three, the thickness of the newly formed tubular dentin increased significantly in both shallow and deep cavity models (Figure 4).

I next investigated whether the CPNE7-induced hard tissue retains the characteristics of physiologic dentin. The presence of dentinal tubules in the newly mineralized area was examined by scanning electron microscopic analysis, and a clear tubule structure was identified along the entire length of predentin (Figure 5A). Masson's trichrome staining revealed that the newly generated dentin area contained a higher collagen content, indicative of recent mineralization activity (Figure 5B). The cytoplasmic regions of odontoblast processes were also distinctly stained within the newly formed dentin. To eliminate the possibility of restorative materials affecting the action of CPNE7, I used composite resin or zinc oxide-eugenol (ZOE) as an alternative cavity filling material. Similarly, CPNE7 treatment led to the formation of tubular dentin, demonstrating its regenerative potential regardless of the restorative material used (Figure 6).

Functional Peptide, Cpne7-DP Directly Penetrates Odontoblastic Cells and Upregulates Odontoblast Differentiation Markers In Vitro

I designed and synthesized an oligopeptide covering the linker region of CPNE7. The amino acid sequence of the oligopeptide was “Lys-Tyr-Lys-Gln-Lys-Arg-Arg-Ser-Tyr-Lys,” and was named as Cpne7-DP (Figure 7). Cpne7-DP was localized to the cytoplasm, and there was no evidence of nuclear labeling (Figure 8A). MTT assay results confirmed that there was no significant difference in cytotoxicity from 0 to 5 days between control and Cpne7-DP-treated groups (Figure 8B). The peptides were diffusely located in the cytoplasm of nucleolin siRNA-transfected cells similar to control, suggesting that Cpne7-DP does not require nucleolin as its receptor (Figure 9). Next, I treated MDPC-23 cells with chlorpromazine (CPZ), an inhibitor of clathrin-mediated endocytosis, or methyl- β -cyclodextrin (MbCD), an inhibitor of caveolin-mediated endocytosis, and examined the localization of Cpne7-DP by immunofluorescence. Cpne7-DP diffusely localized to the cytoplasm in both groups (Figure 10A, 10B). Thus, I concluded that Cpne7-DP does not act through receptor-mediated endocytosis. Treatment with the macropinocytosis inhibitor ethylisopropyl amiloride (EIPA) also showed no effect on the cytoplasmic localization of Cpne7-DP, suggesting that Cpne7-DP is able to directly penetrate odontoblastic cells (Figure 10C). The expression levels of odontoblast marker genes, dentin sialophosphoprotein (dspp), dentin matrix protein 1 (DMP1), and Nestin, increased in hDPCs treated with Cpne7-DP (Figure 11). Cpne7-DP also elevated the DSP expression level compared to control (Figure 12A). Next, I

conducted luciferase reporter assays using a dspp-responsive reporter in mouse dental papilla-derived MDPC-23 cells treated with either rCPNE7 or Cpne7-DP. Treatment of Cpne7-DP increased dspp promoter activity as much as rCPNE7 in a dose-dependent manner, compared to control (Figure 12B). To determine the extent to which Cpne7-DP stimulates mineralization, I examined the mineralization capacity of Cpne7-DP on odontoblast-like cells in vitro. Alizarin red S staining results indicated that Cpne7-DP -treated MDPC-23 cells began to demonstrate mineralized nodule formation on day 7, which significantly increased until day 14. The control group showed fewer mineralized nodules than the Cpne7-DP-treated group microscopically (Figure 13).

Functional Peptide, Cpne7-DP, Promotes Dentin-Like Tissue Formation Ex Vivo

I further evaluated the role of Cpne7-DP by transplanting hDPCs into the subcutaneous tissues of immunocompromised mice using hydroxyapatite/tricalcium phosphate (HA/TCP) under three different conditions: hDPCs only (Control), hDPCs treated with Cpne7-DP, and hDPCs treated with recombinant bone morphogenetic protein 2 (rBMP2). Twelve weeks after the transplantation, the Cpne7-DP treatment group manifested the formation of dentin-pulp-like tissue with cells inserting long cellular processes into the tubule-like structure formed within the newly mineralized tissue. In comparison, the rBMP2 treatment group formed the typical bone-like structure with round-shaped cells entrapped within. Moreover, the formation of bone-marrow-like structures was evident inside the mineralized tissue of the rBMP2 treatment group (Figure 14).

Cpne7-DP Promotes the Regeneration of Tubular Dentin and Dentinal Tubule Occlusion in Shallow and Deep Cavity Models

There has been no peptide reported, which can stimulate physiologic dentin regeneration in vivo. A dentin matrix protein-derived peptide, Cpne7-DP, was first subjected to the assessment of its ability to permeate dentinal tubules. Cpne7-DP labeled with a fluorescent dye was applied by microbrushing onto the pre-exposed dentinal tubules of an extracted tooth for 1 min. After moderate washing, the peptide was observed to flow through the entire length of the dentinal tubules into the pulp by confocal microscopy (Figure 15). I further investigated its function in dentin regeneration in beagle dog tooth defect models. An HIV-1 Tat-derived cell-penetrating peptide was used as control, where its treatment led to no new hard tissue formation. In both shallow and deep cavity models, the treatment of Cpne7-DP resulted in the formation of tertiary dentin underneath the defect after 3 weeks, which retained the tubule structure continuous with that of the remaining dentin (Figure 16A). Furthermore, the thickness of the newly generated dentin was greater when samples were analyzed after 6 weeks (Figure 16B).

Next, I analyzed peritubular dentin formation in beagle tooth defect models by scanning electron microscopy. After removing the filling material, the defect surface where dentinal tubules were exposed by tooth preparation was observed (Figure 17). In the control group where defects received no treatment, a number of exposed tubule openings were seen. The Cpne7-DP treatment group, however, showed much smaller tubule openings, suggesting the possibility that underlying odontoblasts had formed dentin in peritubular

areas as well as in the tubule spaces above their cellular processes. According to the nano-fluid movement test used in the previous study (Park et al. 2019), the Cpne7-DP-treated group demonstrated a significantly smaller volume of liquid flow than the control group (Figure 18).

Cpne7-DP Treatment Promotes Tubular Dentin Regeneration in Pulp Exposure Models

Finally, I generated a pulp exposure model to examine the effect of Cpne7-DP, where odontoblasts undergo consequential cell death. For more detailed histological analysis, it was further divided into three groups: GI cement filling only (Control), GI cement filling after mineral trioxide aggregate (MTA) sealing (MTA group), and GI cement filling after sealing with Cpne7-DP-mixed MTA (Cpne7-DP + MTA group). In the control group, no new hard tissue formation was found at the pulp exposure site, whereas, in the MTA group, a typical bone-like dentin bridge (osteodentin) was newly formed around the exposure site (Figure 20A). As in conventional direct pulp capping using MTA, the osteodentin bridge showed round-shaped cell entrapments within the mineralized tissue. Moreover, hardly any cell alignment was observed under the osteodentin bridge. In the Cpne7-DP + MTA group, on the other hand, dentin bridge with tubular architecture was generated, which had started to close the exposure site (Figure 19A). Furthermore, the palisade layer of odontoblasts expressing DSP and Nestin was well preserved and lined the dentin bridge (Figure 19B).

Table 1. Primer sequences for quantitative reverse transcription polymerase chain reaction

<i>Gene</i>		<i>Sequences (5'-3')</i>
<i>Dspp</i>	Forward	CAACCATAGAGAAAGCAAACGCG
	Reverse	TTTCTGTTGCCACTGCTGGGAC
<i>DMP-1</i>	Forward	ACAGGCAAATGAAGACCC
	Reverse	TTCACTGGCTTGTATGG
<i>Nestin</i>	Forward	AGCCCTGACCACTCCAGTTTATAG
	Reverse	CCCTCTATGGCTGTTTCTTTCTCT
<i>GAPDH</i>	Forward	AGGGCTGCTTTTAACTCTGGT
	Reverse	CCCCTTGATTTTGGAGGGA

Dspp, Dentin sialophosphoprotein; *DMP-1*, Dentin matrix protein-1; *GAPDH*, glyceraldehyde 3-phosphate dehydrogenase

Table 2. List of antibodies for immunoassays.

<i>Antigen</i>	<i>Source</i>	<i>Technique</i>	<i>Dilution</i>	<i>Molecular Weight (kDa)</i>
BSP	Produced as described previously (Lee et al. 2011)	IHC	1:200	35, 70
DSP	Produced as described previously (Lee et al. 2011)	WB, IHC	1:2000, 1:100–200	55
GAPDH	Santa Cruz	WB	1:5000	37
NESTIN	Millipore	WB, IHC	1:1000, 1:200	200
	Thermofisher	IHC	1:100	200

DSP, Dentin sialoprotein; BSP, Bone sialoprotein; GAPDH, glyceraldehyde 3-phosphate dehydrogenase

Table 3. List of reagents and plasmids used.

<i>Reagents</i>	<i>Source</i>
Chlorpromazine	Sigma-Aldrich
Methyl- β -cyclodextrin	Sigma-Aldrich
Ethylisopropyl Amiloride	Sigma-Aldrich
Recombinant CPNE7	Origene
Plasmids	Source
Control siRNA	Ambion
Nucleolin-targeting siRNA	Ambion

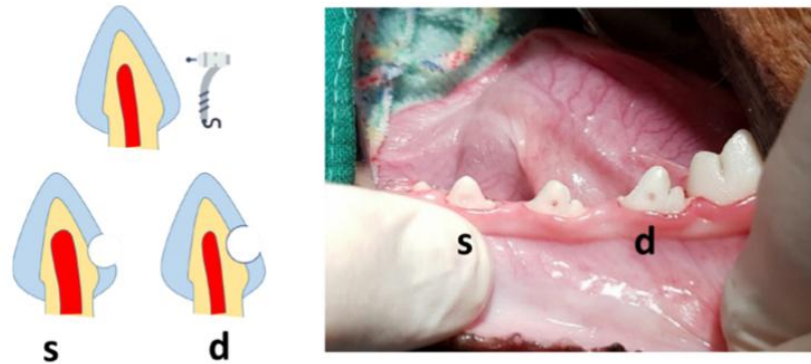


Figure 1. Schematic illustration and representative macroscopic image of s) shallow and d) deep cavity prepared on the cervical areas of beagle dog premolars.

Dentinal defects were generated with a high-speed #4 round bur on the cervical areas of beagle dog premolars. For shallow cavity, the drilling was stopped just before the half of the bur penetrated, and for deep cavity, the drilling was stopped when the underlying pulp started to show through as bluish-grey color.

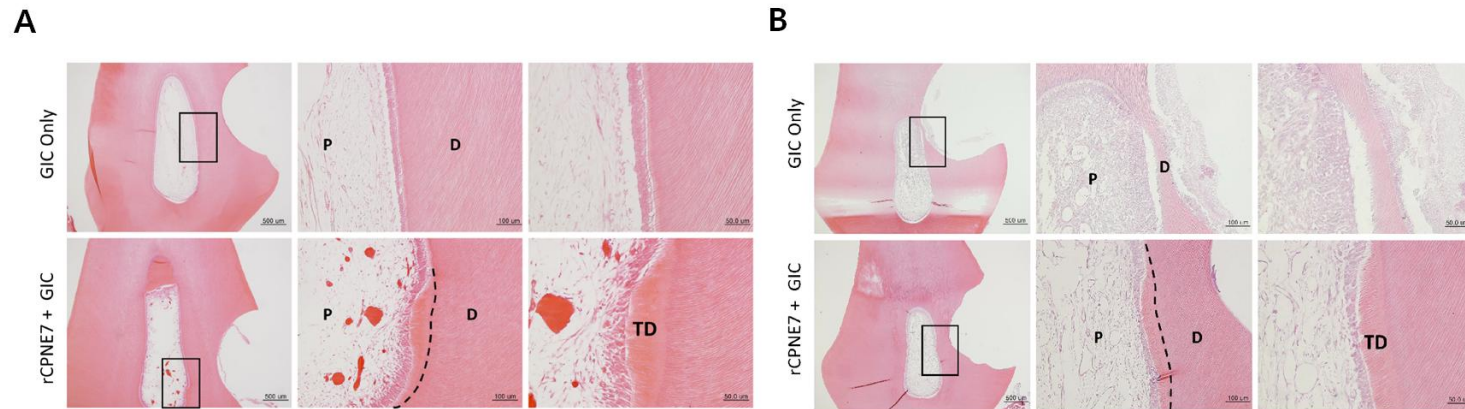


Figure 2. Histological analysis three weeks after the *in vivo* treatment of rCPNE7.

(A) Histological analysis of dental pulp responses at the shallow cavity preparation areas treated with or without rCPNE7 by hematoxylin and eosin staining after 3 weeks. (n = 6). Dashed line indicates the remaining original dentin/newly formed dentin interfaces. (B) Histological analysis of dental pulp responses at the deep cavity preparation areas with or without rCPNE7 treatment by hematoxylin and eosin staining after 3 weeks. (n = 6). Dashed line indicates the remaining original dentin/newly formed dentin interfaces. P, pulp; D, dentin; TD, newly formed tertiary dentin.

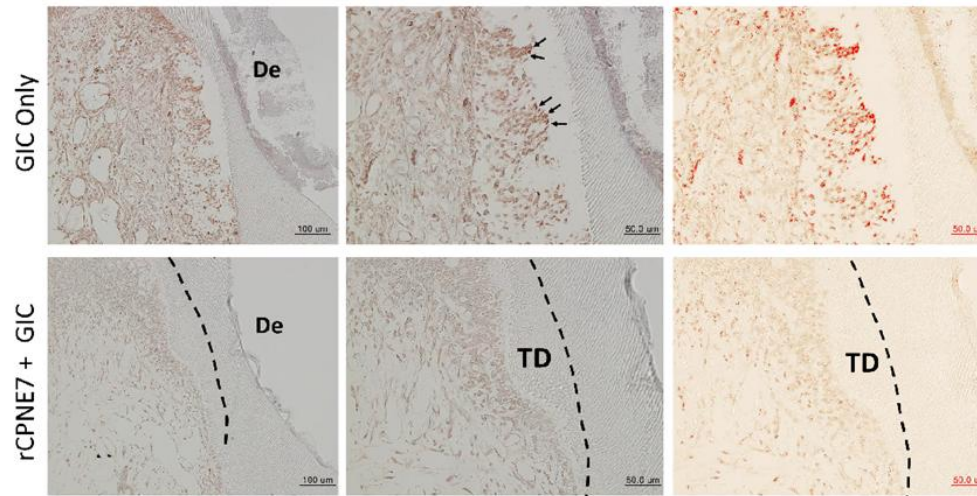


Figure 3. TUNEL staining of dental pulp at the deep cavity preparation areas with or without rCPNE7 treatment.

Terminal deoxynucleotidyl transferase dUTP nick end labeling (TUNEL) staining was performed in the deep cavity model to examine the pulp cell population survival beneath the dentinal defects generated. Positive TUNEL signals were converted to red color using IHC Profiler of Image J software. TD, newly formed tertiary dentin; De, defect.

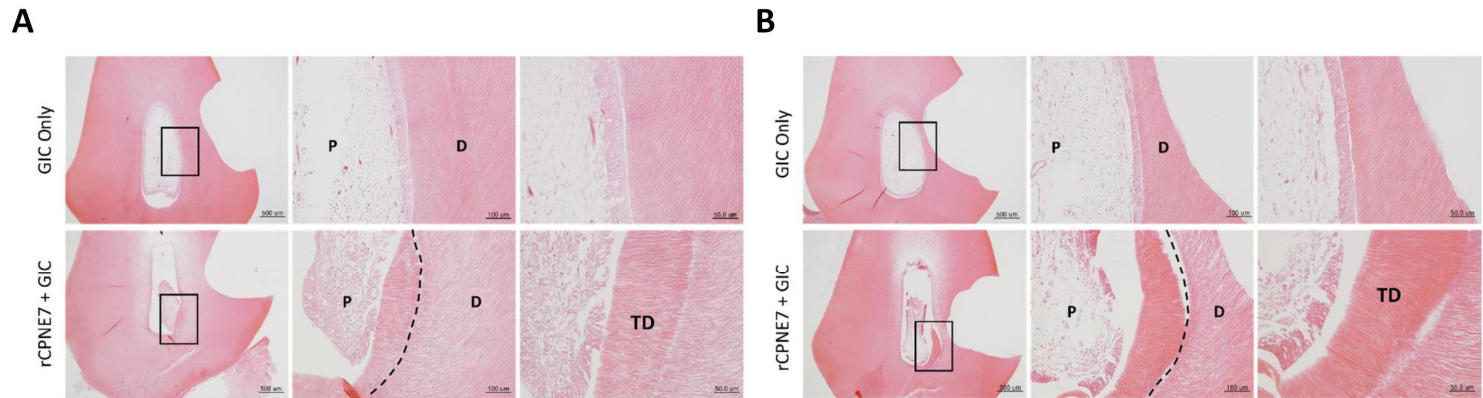


Figure 4. Histological analysis six weeks after the *in vivo* treatment of rCPNE7.

(A) Histological analysis of dental pulp responses at the shallow cavity preparation areas treated with or without rCPNE7 by hematoxylin and eosin staining after 6 weeks. (n = 6). Dashed line indicates the remaining original dentin/newly formed dentin interfaces. (B) Histological analysis of dental pulp responses at the deep cavity preparation areas with or without rCPNE7 treatment by hematoxylin and eosin staining after 6 weeks. (n = 6). Dashed line indicates the remaining original dentin/newly formed dentin interfaces. P, pulp; D, dentin; TD, newly formed tertiary dentin.

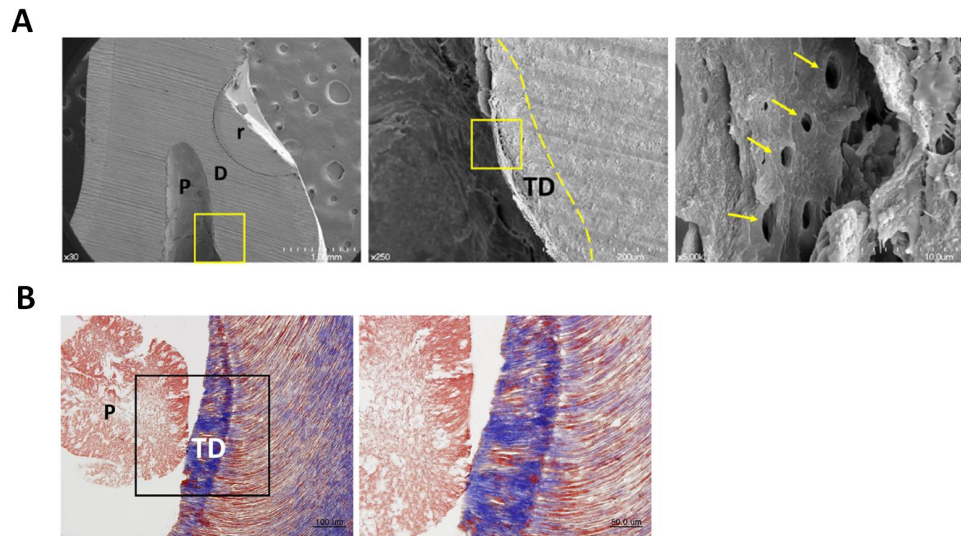


Figure 5. The CPNE7-induced hard tissue retains the dentinal tubule structure.

(A) Dentinal tubule structure within the newly generated tertiary dentin in rCPNE7-treated group was observed by scanning electron microscope. Boxed areas indicate the dentin–pulp interface in the newly formed dentin. Arrows indicate the dentinal tubules; dashed line indicates the remaining original dentin/newly formed dentin interfaces. (B) Masson's trichrome staining of newly formed dentin in rCPNE7-treated group. P, pulp; D, dentin; TD, newly formed tertiary dentin; r, resin composite.

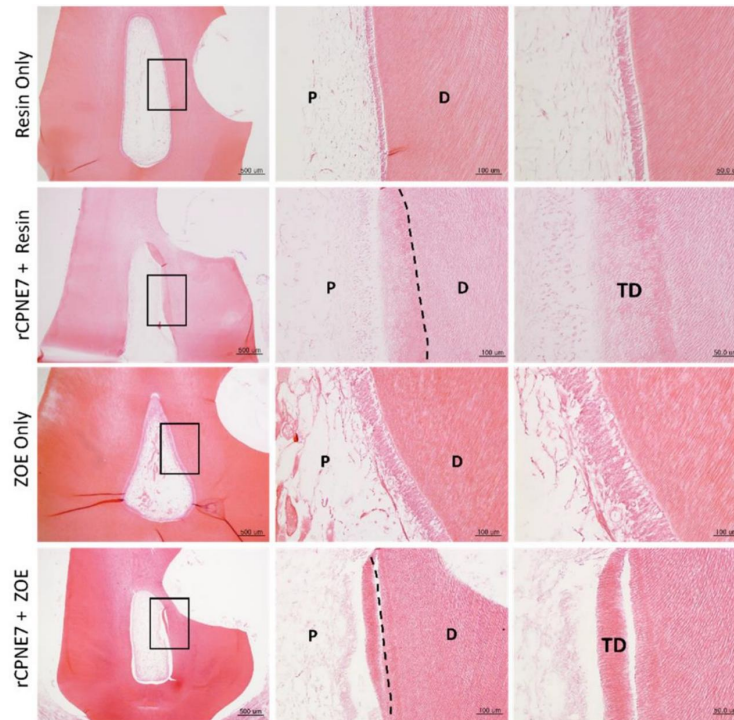


Figure 6. Tertiary dentin formation is not dependent on the restorative material used.

Histological analysis of dental pulp responses at the cavity preparation areas treated with or without rCPNE7 followed by composite resin or ZOE filling after six weeks by hematoxylin and eosin staining (n = 6). Dashed line indicates the remaining original dentin/newly formed dentin interfaces. P, pulp; D, dentin; TD, newly formed tertiary dentin.

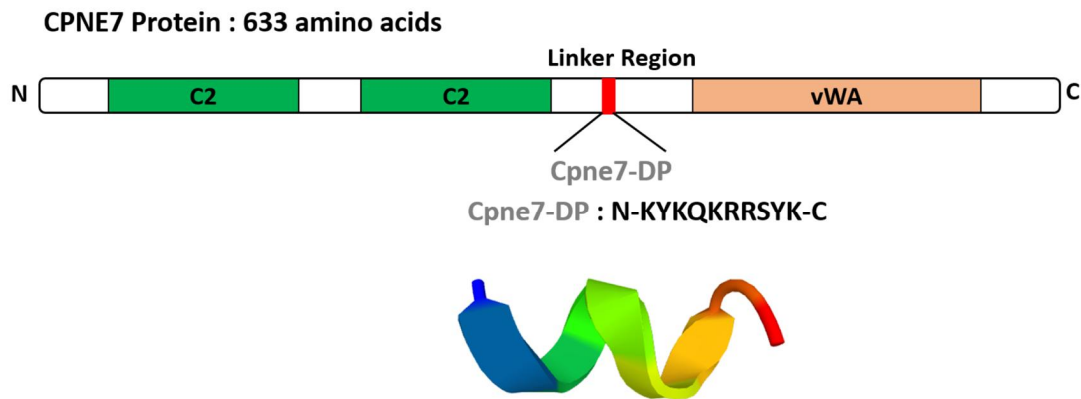


Figure 7. Amino acid sequence and ribbon structure of Cpne7-DP derived from the linker region of CPNE7 protein.

Cpne7-DP consists of a synthetic peptide corresponding to the 10 amino acid residue 344–353 fragment (Lys-Tyr-Lys-Gln-Lys-Arg-Arg-Ser-Tyr-Lys) of the hCPNE7 protein. The purity was greater than 97% as determined by high-performance liquid chromatography.

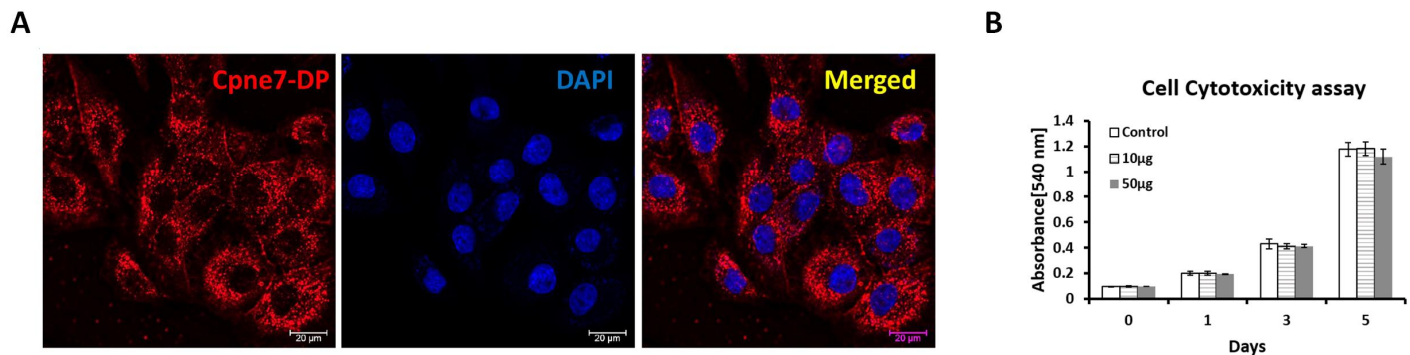


Figure 8. Intracellular distribution and cytotoxicity of Cpne7-DP in odontoblastic MDPC-23 cells.

(A) To investigate the localization of Cpne7-DP (red) in odontoblastic MDPC-23 cells, MDPC-23 cells were treated with Cy5-labeled Cpne7-DP (10 $\mu\text{g/mL}$) and fixed 3 h later. The detection was visualized by immunofluorescence.

(B) The effect of Cpne7-DP on the proliferation of hDPCs was evaluated using an MTT (3-(4,5-dimethylthiazol-2-yl)-2,5-diphenyl tetrazolium bromide) assay. All values represent the mean \pm standard deviation of triplicate experiments. DAPI, 4', 6-diamidino-2-phenylindole.

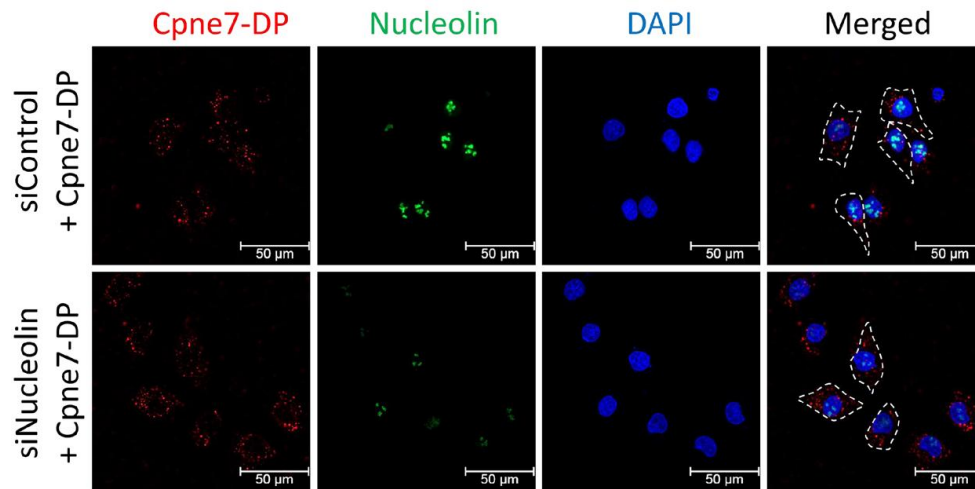


Figure 9. Cpne7-DP does not require Nucleolin as its cell surface receptor.

Internalization of Cpne7-DP detected by immunofluorescence in MDPC-23 cells after treatment with nucleolin siRNA. MDPC-23 cells were pre-treated with nucleolin siRNA for 1 h before Cpne7-DP treatment. DAPI, 4', 6-diamidino-2-phenylindole.

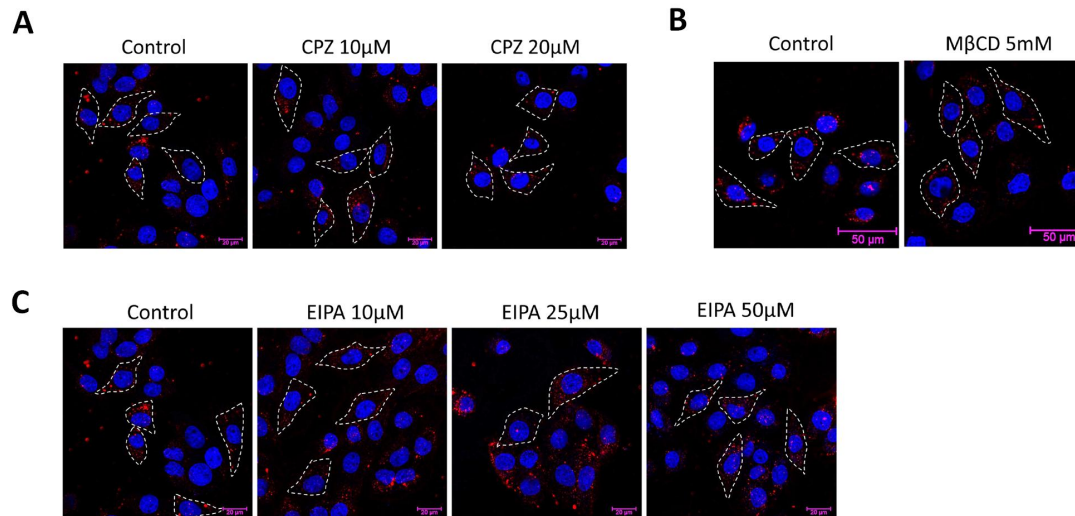


Figure 10. Functional peptide, Cpne7-DP directly penetrates odontoblastic cells.

(A) Internalization of Cpne7-DP detected by immunofluorescence in MDPC-23 cells pre-treated with varying concentration of chlorpromazine (CPZ; 10 and 20 μM) for 1 h before Cpne7-DP treatment. (B) Internalization of Cpne7-DP detected by immunofluorescence in MDPC-23 cells pre-treated with methyl-beta-cyclodextrin (MβCD) for 1 h before Cpne7-DP treatment. (C) Internalization of Cpne7-DP detected by immunofluorescence in MDPC-23 cells pre-treated with ethylisopropyl amiloride (EIPA) for 1 h before Cpne7-DP treatment. Dashed line indicates the cell edge.

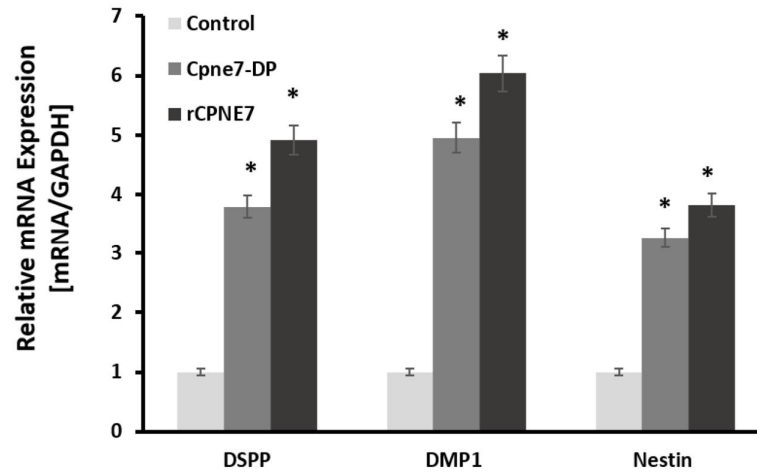


Figure 11. Functional peptide, Cpne7-DP, upregulates odontoblast differentiation marker genes *in vitro*.

Real-time PCR analysis of DSPP, DMP1, and Nestin mRNA in hDPCs treated with Cpne7-DP or rCPNE7. All values represent the mean \pm standard deviation of triplicate experiments. * $p < 0.05$ compared with control. GAPDH, glyceraldehyde 3-phosphate dehydrogenase.

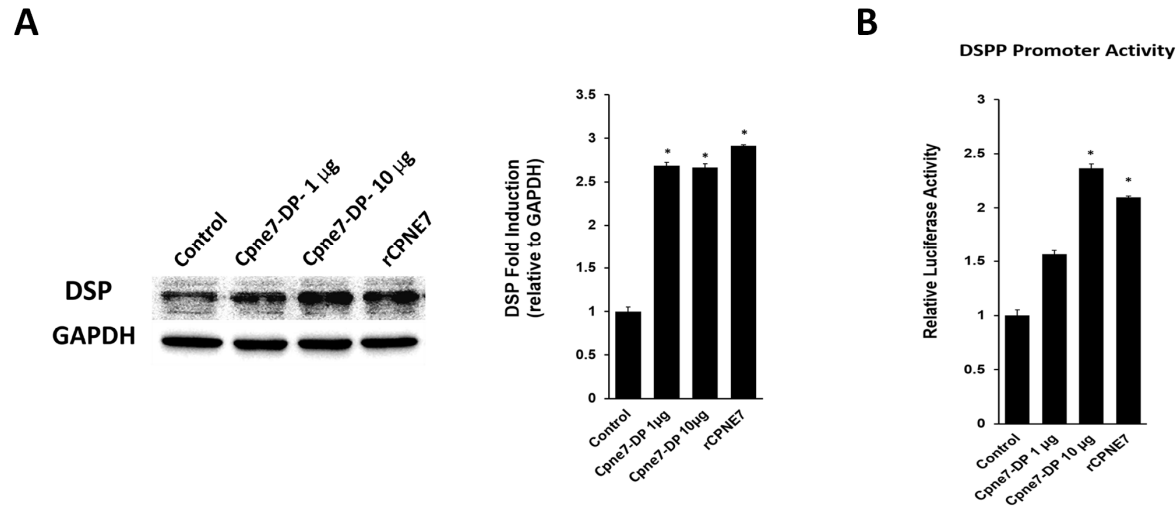


Figure 12. Functional peptide, Cpne7-DP, upregulates odontoblast differentiation marker protein and dspp promoter activity *in vitro*.

(A) Western blotting and semi-quantification analysis of DSP expression in hDPCs treated with Cpne7-DP 1 µg, 10 µg or rCPNE7. (B) Transcriptional activity of dentin sialophosphoprotein (dspp) promoter was evaluated by luciferase assay in MDPC-23 cells treated with Cpne7-DP 1 µg, 10 µg or rCPNE7. All values represent the mean ± standard deviation of triplicate experiments. * $p < 0.05$ compared with control. GAPDH, glyceraldehyde 3-phosphate dehydrogenase.

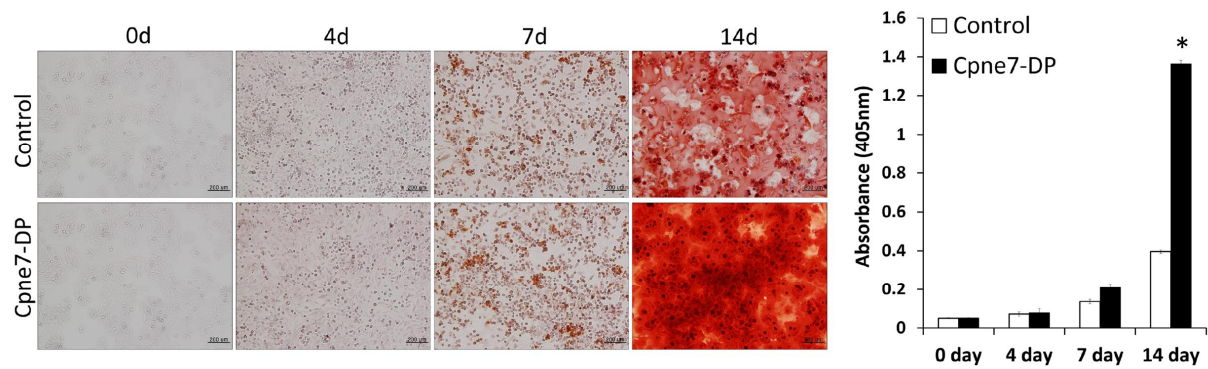


Figure 13. Functional peptide, Cpne7-DP, stimulates mineralization activity of odontoblastic cells *in vitro*.

The mineralized nodule formation in MDPC-23 cells cultured in differentiation medium for 14 days with or without Cpne7-DP was analyzed by alizarin red S staining and corresponding semi-quantification on days 0, 4, 7, and 14.

* $p < 0.05$ compared with control.

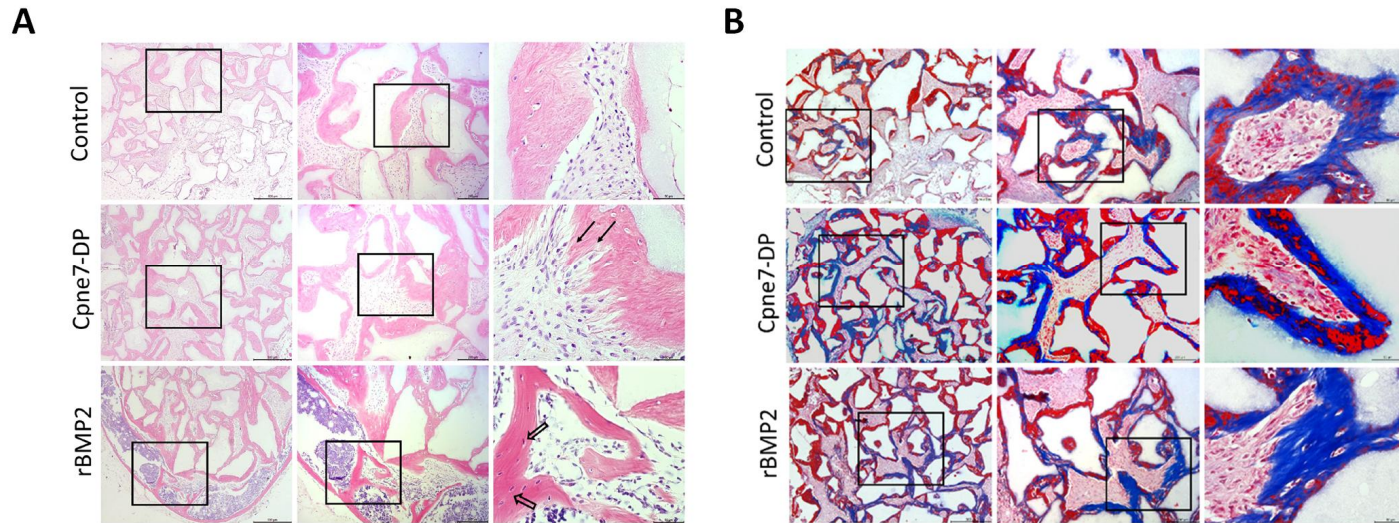


Figure 14. Functional Peptide, Cpne7-DP, Promotes Dentin-Like Tissue Formation *ex vivo*.

(A) Histological analysis of the subcutaneously transplanted 100 mg HA/TCP particles alone or with Cpne7-DP or rBMP2 in a 0.5% fibrin gel into immunocompromised mice for 12 weeks. Samples were stained with hematoxylin-eosin. Arrows indicate dentinal tubule-like structures; empty arrows indicate lacunae-containing osteocyte-like cells. (B) Masson's trichrome staining of the subcutaneously transplanted 100 mg HA/TCP particles alone or with Cpne7-DP or rBMP2 in a 0.5% fibrin gel into immunocompromised mice for 12 weeks.

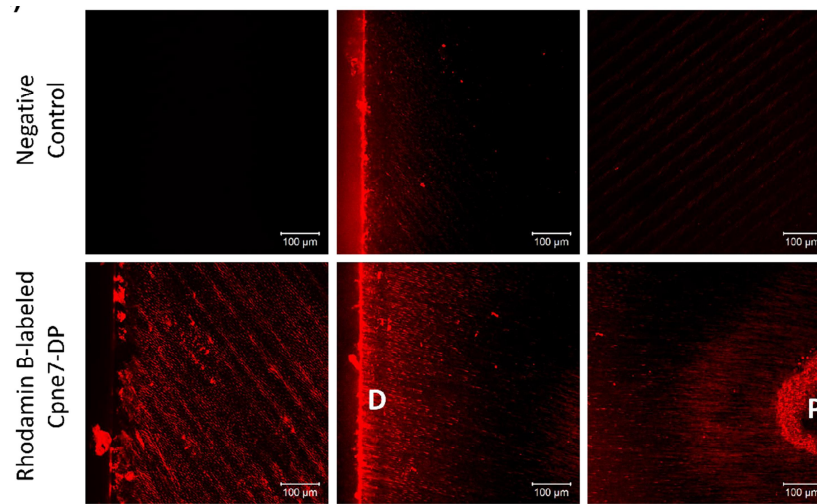


Figure 15. Assessment of the ability of Cpne7-DP to permeate dentinal tubules.

Evaluation of dentinal tubule penetration of Rhodamin B-labeled Cpne7-DP by using confocal laser scanning microscopy. Cpne7-DP labeled with a fluorescent dye was applied by microbrushing onto the pre-exposed dentinal tubules of an extracted tooth for 1 min.

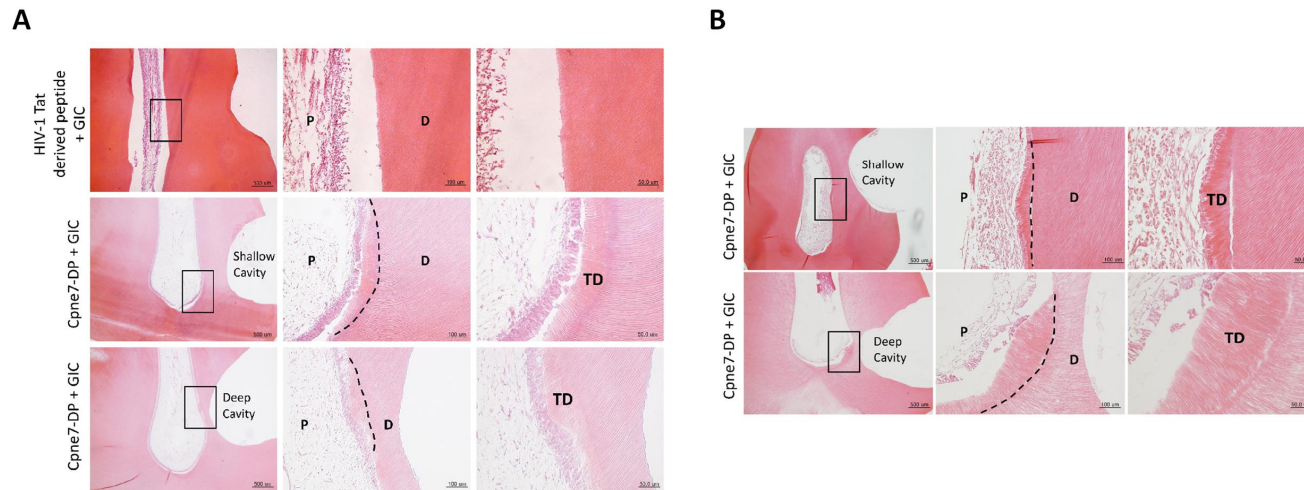


Figure 16. Histological analysis three or six weeks after *in vivo* treatment of Cpne7-DP.

(A) Histological analysis of dental pulp responses at the shallow cavity and deep cavity preparation areas treated with HIV-1 Tat-derived peptide (Control) or Cpne7-DP after 3 weeks by hematoxylin and eosin staining (n = 12). Dashed lines indicate the remaining original dentin/newly formed dentin interfaces. (B) Histological analysis of dental pulp responses at the shallow cavity and deep cavity preparation areas treated with Cpne7-DP after six weeks by hematoxylin and eosin staining (n = 6). Dashed line indicates the remaining original dentin/newly formed dentin interfaces. P, pulp; D, dentin; TD, newly formed tertiary dentin.

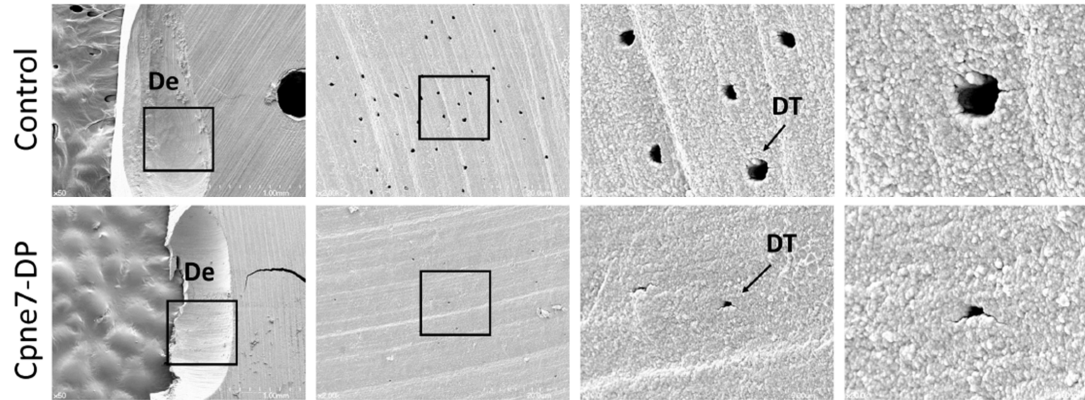


Figure 17. Cpne7-DP treatment promotes dentinal tubule occlusion by inducing peritubular dentin formation.

Scanning electron microscopic analysis of cross-sectioned surface between the defect and the pulp space. Areas noted by a and b indicate sectioned surfaces underneath the unaffected part of the crown and underneath the defect, respectively. De, defect; DT, dentinal tubules.

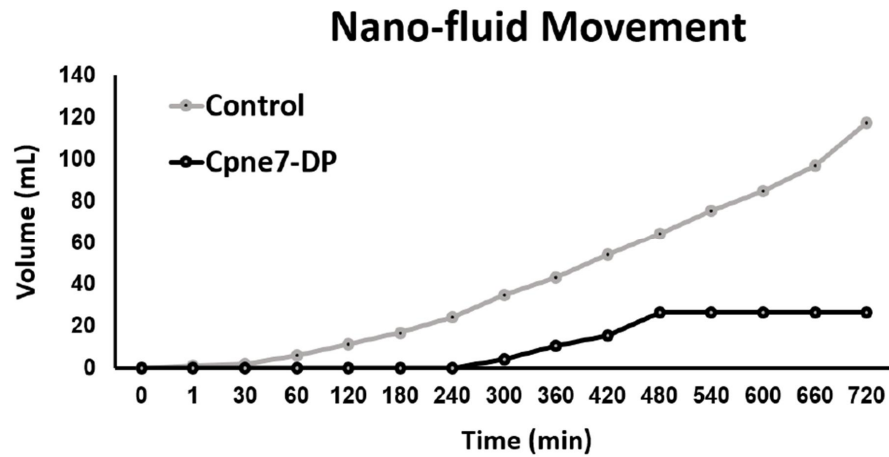


Figure 18. Nano-fluid movement (microleakage) analysis.

To investigate the extent of tubule occlusion, nano-fluid measuring device was used that recognizes the movement of bubbles generated when distilled water is left to flow from the tooth apex to the exposed dentin at 70 cm H₂O.

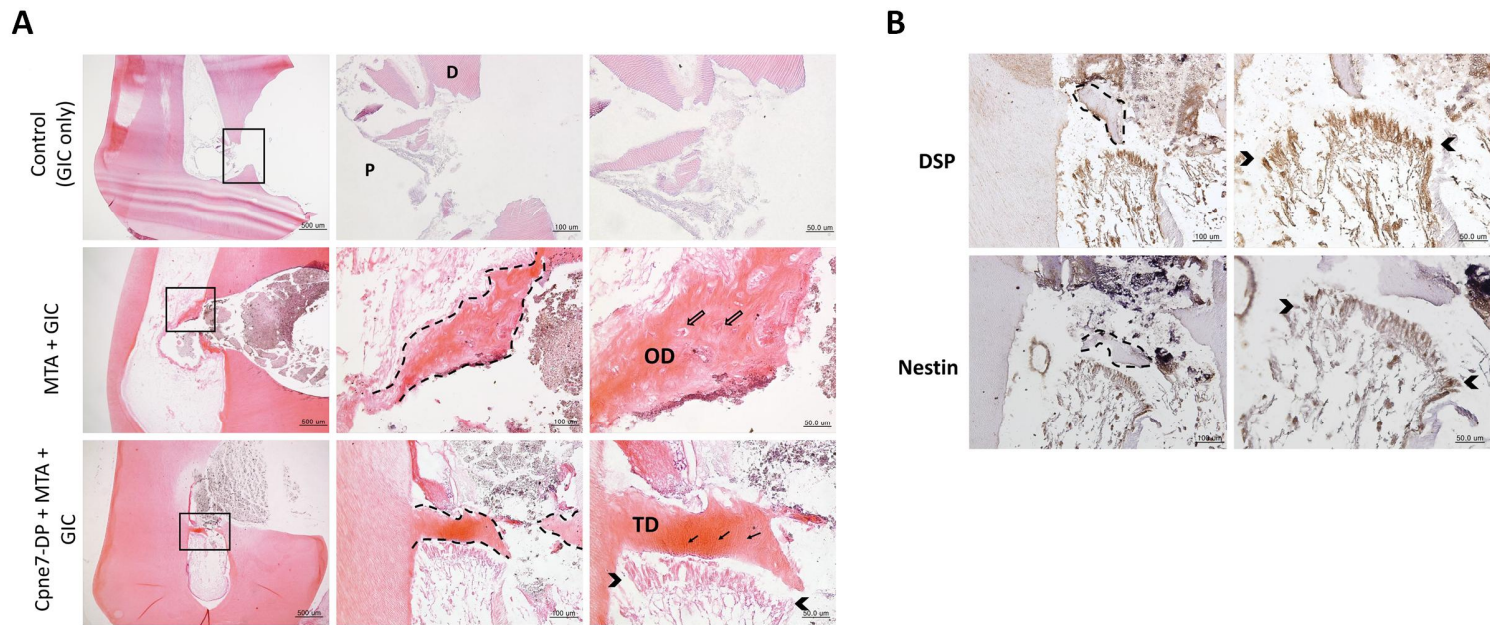


Figure 19. Cpne7-DP treatment promotes the regeneration of tubular orthodontin in pulp exposure canine models.

(A) Histological analysis of dental pulp responses at the complete pulp exposure areas filled with glass ionomer (GI) cement only, or sealed with MTA before GI cement filling, or sealed with MTA dissolved in Cpne7-DP before GI

cement filling. Samples were analyzed by hematoxylin and eosin staining after 12 weeks (n = 6). (B) Immunohistochemical staining of cells underlying the newly formed dentin bridge in (A) with anti DSP (1:100) and anti-Nestin (1:100) in the pulp exposure model treated with Cpne7-DP. Empty arrows indicate the lacunae containing osteocytes; arrows indicate the dentinal tubules. Dashed line indicates the newly formed dentin bridge edge. Brackets outline the newly differentiated odontoblast layer. P, pulp; D, dentin; TD, newly formed tertiary dentin; OD, osteodentin.

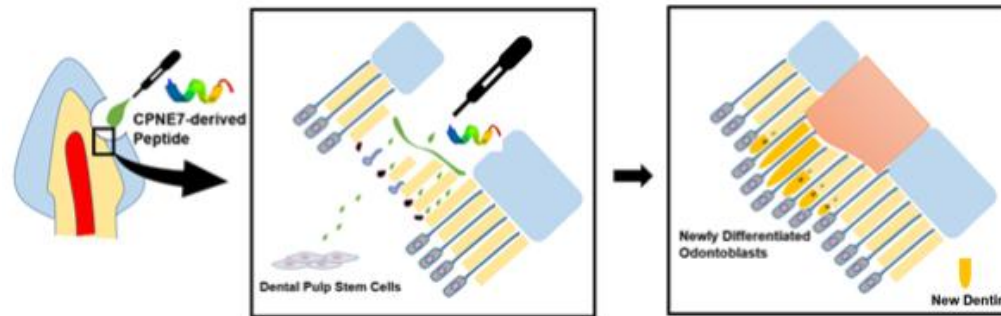


Figure 20. Schematic illustration of CPNE7 acting in two different ways to regenerate tubular dentin.

In cases of a mild stimulus followed by shallow dentinal defects, treatment of CPNE7 leads to the reactivation of underlying resting-state mature odontoblasts to resume active matrix secretion. Under severe stimulus followed by deep dentinal defects that majorly damage underlying odontoblasts, treatment of CPNE7 promotes differentiation of new odontoblasts from the pulp cell population, which can insert their cellular processes into the remaining dentinal tubules and form a tertiary dentin structure.

IV. Discussion

Dentin has a number of similarities with bone both in its chemical composition and its mode of formation; however, it does not undergo lifelong remodeling and cannot be replaced after loss (Goldberg et al. 2011; Veis 1993). Odontoblasts are ectomesenchyme-derived post-mitotic cells that are responsible for dentin development and eventually line dentin (Ruch et al. 1995). Although odontoblasts have recently been reported to have sensory and immune cell capacities (Okumura et al. 2005; Veerayutthwilai et al. 2007), their primary role is the secretion of the organic matrix that will be progressively mineralized (Butler and Ritchie 2003). Noticeably, odontoblasts elongate their cellular processes as they secrete and form predentin. These odontoblastic processes ultimately get embedded in the mineralized dentin matrix, establishing the dentinal tubule structure (Holland 1985). The secretory activity of a mature odontoblast that has completed primary and secondary dentin formation diminishes under healthy conditions. These resting state odontoblasts typically shrink in size and accumulate lipofuscin due to decreased autophagic activity (Couve et al. 2013). In response to dentinal defects, either underlying odontoblasts are reactivated to generate physiologic reactionary dentin or other pulp cell sources are recruited and differentiate into odontoblast-like cells to produce pathologic reparative dentin (Smith et al. 2003). These endogenous processes may be a key to regenerative medicine for tooth dentin.

Shallow and mild injuries to dentin stimulate the matrix-secreting activity of underlying resting state odontoblasts. The newly formed tertiary dentin is

continuous with remaining dentin through the dentinal tubule structure and is called “reactionary” dentin (Smith et al. 2003). In the case of deep and severe dentin injuries, underlying odontoblasts partially or massively undergo cell apoptosis, and a sub-odontoblastic population is recruited to differentiate into odontoblast-like cells (Foreman and Barnes 1990; Hu et al. 1998; Park et al. 2020). Whether these pulp cells have really differentiated into odontoblasts can be examined by the morphology of the newly generated mineralized tissue called “reparative dentin.” In the present study, treatment of CPNE7 or its derivative peptide Cpne7-DP resulted in the regeneration of tubular dentin in both the shallow and deep cavity models, indicating their abilities to not only promote new odontoblast differentiation, but to reactivate the matrix-secretion of underlying odontoblasts.

In addition to causing hypersensitivity, exposed dentinal tubules can be a route for the invasion of foreign substances (Michelich et al. 1980). The current treatment for dentin hypersensitivity patients incorporates insoluble precipitate formation in the open tubules (Hiatt and Johansen 1972; Pashley 1986). The ability of Cpne7-DP to stimulate underlying odontoblasts to resume matrix-secreting activity results in peritubular dentin formation. In addition to the newly generated tubular dentin along the pulp side, the SEM analysis revealed that peritubular dentin is deposited above the odontoblast process near the dentin-restoration interface. Consequently, it resulted in the physiologic occlusion of dentinal tubules. Integrity of the tubule occlusion was further confirmed by a nano-fluid movement test.

A number of synthetic peptides, especially those derived from proteins in an enamel or dentin matrix, have been developed to promote

reminerization of enamel and dentin (Cao et al. 2014; Gulseren et al. 2018; Lv et al. 2015; Wang et al. 2018). Most were capable of inducing hydroxyapatite deposition, and a DSP-derived peptide was reported to act on pulp cells and induce osteodentin formation (Kim et al. 2009). In the present study, Cpne7-DP highly reproduced the *in vitro* effects of CPNE7 by upregulating odontoblast marker genes, DSPP, and Nestin. Moreover, subcutaneous transplantation of Cpne7-DP-treated hDPCs resulted in the formation of a dentin-pulp-like complex *ex vivo*. Unlike CPNE7, which is internalized via nucleolin-mediated endocytosis, Cpne7-DP seems to act on odontoblasts by directly penetrating the cell membrane. Exactly how odontoblast marker gene transcription is regulated by Cpne7-DP is an area of future exploration.

Although the efficiency of hard tissue regeneration differs in model animals, regeneration studies in large mammals (e.g., dogs) have been reported to be more challenging than in small animals (e.g., mice) (Farah et al. 2016; Kantarci et al. 2015). Nevertheless, large mammals provide a more appropriate model for mimicking human disease and are thus more transferable to a human model. In the canine model, both CPNE7 and Cpne7-DP showed successful regeneration of tubular dentin. As the results were based on a single topical application, the effects of multiple repetitive applications should also be analyzed to determine their additive effects. The thickness of the newly formed tubular dentin increased with time, and 6-week samples demonstrated greater new dentin volume than 3-week samples. Such correlation implies that the secretory activity of either newly differentiated odontoblast-like cells or existing odontoblasts is prolonged once

triggered. Nonetheless, one of the limitations of this study includes the lack of an exact quantification of newly formed tertiary dentin.

The findings of the current study suggest that Cpne7-DP promotes the formation of new tubular dentin by inducing odontoblast differentiation of dental pulp stem cells in both dentin and pulp exposure models (Figure 20). The development of Cpne7-DP, a synthetic oligopeptide derived from CPNE7, proved to be advantageous not only in that it perfectly reproduces the functions of CPNE7, but it is a more stable and potent cell-penetrating peptide. Coherent observations in *in vitro*, *ex vivo*, and *in vivo* models establish the groundwork for the clinical translation of Cpne7-DP, which shows a promising ability to arrest the demineralization process, compensate for lost dentin in dentin defects, and occlude exposed dentinal tubules to reduce dentin hypersensitivity.

V. Conclusions

Treatment of tooth defects has been largely dependent on mechanically removing the unhealthy part and replacing it with solid dental materials. Due to the limitations of the dental materials such as post-operative hypersensitivity and secondary caries, biological repair of dentin has become a field of growing interest. Most of the previously reported bioactive molecules lead to repair with bone-like tissue, which is considered sufficient to seal the exposed dental pulp but lacks various protective roles of native dentin. In this study, potential application of Copine 7-derived oligopeptide for regenerative dental therapeutics is thoroughly evaluated.

- 1) Cpne7-DP directly penetrates odontoblastic cells and upregulates odontoblast differentiation markers, while stimulating mineralization nodule formation in odontoblastic MDPC-23 cells *in vitro*.
- 2) Treatment of Cpne7-DP promotes dentin-pulp complex-like tissue formation *ex vivo* as confirmed by the subcutaneous transplantation study.
- 3) Cpne7-DP can permeate dentinal tubules.
- 4) Cpne7-DP treatment promotes the regeneration of tubular dentin and dentinal tubule occlusion in shallow and deep cavity canine models.
- 5) Cpne7-DP treatment promotes the regeneration of tubular dentin in pulp exposure canine models.

VI. References

- Butler WT, Ritchie H. 2003. The nature and functional significance of dentin extracellular matrix proteins. *International Journal of Developmental Biology*. 39(1):169-179.
- Cao Y, Liu W, Ning T, Mei ML, Li Q-L, Lo EC, Chu C. 2014. A novel oligopeptide simulating dentine matrix protein 1 for biomimetic mineralization of dentine. *Clinical oral investigations*. 18(3):873-881.
- Choung H, Lee D, Lee J-H, Shon W, Lee J-H, Ku Y, Park J. 2016. Tertiary dentin formation after indirect pulp capping using protein cpne7. *Journal of dental research*. 95(8):906-912.
- Couve E, Osorio R, Schmachtenberg O. 2013. The amazing odontoblast: Activity, autophagy, and aging. *Journal of dental research*. 92(9):765-772.
- Farah Z, Fan H, Liu Z, He J-Q. 2016. A concise review of common animal models for the study of limb regeneration. *Organogenesis*. 12(3):109-118.
- Foreman P, Barnes I. 1990. A review of calcium hydroxide. *International endodontic journal*. 23(6):283-297.
- Goldberg M, Kulkarni AB, Young M, Boskey A. 2011. Dentin: Structure, composition and mineralization: The role of dentin ecm in dentin formation and mineralization. *Frontiers in bioscience (Elite edition)*. 3:711.
- Gronthos S, Brahim J, Li W, Fisher L, Cherman N, Boyde A, DenBesten P, Robey PG, Shi S. 2002. Stem cell properties of human dental pulp stem cells. *Journal of dental research*. 81(8):531-535.
- Gulseren G, Tansik G, Garifullin R, Tekinay AB, Guler MO. 2018. Dentin phosphoprotein mimetic peptide nanofibers promote biomineralization. *Macromolecular bioscience*.1800080.
- Hahn C-L, Best A. 2006. The pulpal origin of immunoglobulins in dentin

- beneath caries: An immunohistochemical study. *Journal of endodontics*. 32(3):178-182.
- Hiatt WH, Johansen E. 1972. Root preparation i. Obturation of dentinal tubules in treatment of root hypersensitivity. *Journal of periodontology*. 43(6):373-380.
- Holland G. 1985. The odontoblast process: Form and function. *Journal of dental research*. 64(4):499-514.
- Hosoya A, Nakamura H, Akahane S, Yoshida K, Yoshida N, Ninomiya T, Hoshi K, Sahara N, Kasahara E, Ozawa H. 2006. Immunohistochemical study of osteodentin in the unerupted rat incisor. *Journal of Oral Biosciences*. 48(2):132-137.
- Hu C-C, Zhang C, Qian Q, Tatum NB. 1998. Reparative dentin formation in rat molars after direct pulp capping with growth factors. *Journal of endodontics*. 24(11):744-751.
- Kantarci A, Hasturk H, Van Dyke TE. 2015. Animal models for periodontal regeneration and peri-implant responses. *Periodontology* 2000. 68(1):66-82.
- Kim J-H, Hong J-B, Lim B-S, Cho B-H. 2009. Histological evaluation of direct pulp capping with dsp-derived synthetic peptide in beagle dog. *Journal of Korean Academy of Conservative Dentistry*. 34(2):120-129.
- Kim SG. 2017. Biological molecules for the regeneration of the pulp-dentin complex. *Dental Clinics*. 61(1):127-141.
- Langeland K. 1987. Tissue response to dental caries. *Dental Traumatology*. 3:149-171
- Lee I-B, Kim M-H, Kim S-Y, Chang J-H, Cho B-H, Son H-H, Back S-H. 2008. Development of nano-fluid movement measuring device and its application to hydrodynamic analysis of dentinal fluid. *Restorative Dentistry and Endodontics*. 33(2):141-147.
- Lee J-H, Lee D-S, Choung H-W, Shon W-J, Seo B-M, Lee E-H, Cho J-Y, Park J-C. 2011. Odontogenic differentiation of human dental pulp stem cells induced by preameloblast-derived factors. *Biomaterials*. 32(36):9696-9706.

- Lv X, Yang Y, Han S, Li D, Tu H, Li W, Zhou X, Zhang L. 2015. Potential of an amelogenin based peptide in promoting remineralization of initial enamel caries. *Archives of oral biology*. 60(10):1482-1487.
- Maita E, Simpson M, Tao L, Pashley DH. 1991. Fluid and protein flux across the pulpodentine complex of the dog in vivo. *Archives of oral biology*. 36(2):103-110.
- Michelich V, Schuster G, Pashley DH. 1980. Bacterial penetration of human dentin in vitro. *Journal of Dental Research*. 59(8):1398-1403.
- Nagaoka S, Miyazaki Y, Liu H-J, Iwamoto Y, Kitano M, Kawagoe M. 1995. Bacterial invasion into dentinal tubules of human vital and nonvital teeth. *Journal of Endodontics*. 21:70-73.
- Oh H-J, Choung H-W, Lee H-K, Park S-J, Lee J-H, Lee D-S, Seo B-M, Park J-C. 2015. Cpne7, a preameloblast-derived factor, regulates odontoblastic differentiation of mesenchymal stem cells. *Biomaterials*. 37:208-217.
- Okumura R, Shima K, Muramatsu T, Nakagawa K-i, Shimono M, Suzuki T, Magloire H, Shibukawa Y. 2005. The odontoblast as a sensory receptor cell? The expression of trpv1 (vr-1) channels. *Archives of histology and cytology*. 68(4):251-257.
- Park S, Lee Y, Lee D, Park J, Kim R, Shon WJJoDR. 2019a. Cpne7 induces biological dentin sealing in a dentin hypersensitivity model. 98(11):1239-1244.
- Park Y-H, Lee YS, Park J-S, Kim SH, Bae HS, Park J-C. 2019b. Expression of cpne7 during mouse dentinogenesis. *Journal of Molecular Histology*. 50(3):179-188.
- Park Y, Lee Y, Seo Y, Seo H, Park J, Bae H, Park J. 2020. Midkine promotes odontoblast-like differentiation and tertiary dentin formation. *Journal of Dental Research*.0022034520925427.
- Pashley DH. 1979. The influence of dentin permeability and pulpal blood flow on pulpal solute concentrations. *Journal of endodontics*. 5(12):355-361.

- Pashley DH. 1986. Dentin permeability, dentin sensitivity, and treatment through tubule occlusion. *Journal of Endodontics*. 12(10):465-474.
- Pitts N. 2004. Are we ready to move from operative to non-operative/preventive treatment of dental caries in clinical practice? *Caries Research*. 38:294-304.
- Ruch J, Lesot H, Begue-Kirn C. 1995. Odontoblast differentiation. *The International journal of developmental biology*. 39(1):51-68.
- Smith AJ, Cassidy N, Perry H, Begue-Kirn C, Ruch J-V, Lesot H. 2003. Reactionary dentinogenesis. *International Journal of Developmental Biology*. 39(1):273-280.
- Tomsig J, Creutz C. 2002. Copines: A ubiquitous family of Ca^{2+} -dependent phospholipid-binding proteins. *Cellular and Molecular Life Sciences CMLS*. 59(9):1467-1477.
- Veerayutthwilai O, Byers M, Pham TT, Darveau R, Dale B. 2007. Differential regulation of immune responses by odontoblasts. *Oral microbiology and immunology*. 22(1):5-13.
- Weis A. 1993. Mineral-matrix interactions in bone and dentin. *Journal of Bone and Mineral Research*. 8(S2):S493-S497.
- Wang K, Wang X, Li H, Zheng S, Ren Q, Wang Y, Niu Y, Li W, Zhou X, Zhang L. 2018. A statherin-derived peptide promotes hydroxyapatite crystallization and in situ remineralization of artificial enamel caries. *RSC Advances*. 8(3):1647-1655.

국문초록

CPNE7 유래 기능성 펩타이드를 이용한 세관상아질의 재생

이윤선

서울대학교 대학원

치의과학과 세포 및 발생 생물학 전공

(지도교수 박 주 철)

재료과학 및 줄기세포 생물학 연구의 점진적인 발전으로 재생 치의학 분야에서 역시 큰 학문적 도약이 이루어지고 있다. 하지만 아직까지는 재생된 조직이 본래의 구조와 기능을 얼마나 유지하는지에 대한 질적인 평가보다는 경조직 재생 성공 여부 자체가 치아 재생 연구에서의 주된 관심사이다. 특히 치아 상아질과 골은 구조와 기능이 분명 다르지만 그 구성 성분이 매우 유사하여 상아질 재생 연구에 있어 골조직과의 구분은 크게

고려되지 않아왔다.

본 논문에서는 Copine 7 (CPNE7) 단백질에서 합성한 기능성 펩타이드 Cpne7-DP를 소개하고, 그 기능을 *in vitro*, *ex vivo*, 그리고 *in vivo* 실험을 통해 분석하였다. 사람치수세포와 생쥐의 조상아세포주가 생체 외 Cpne7-DP 처리 실험에 이용되었으며, 비글견 치아 손상 모델이 생체내 상아질 재생 확인에 이용되었다. 관주공간의 폐쇄 여부는 주사전자현미경과 미세누출 실험을 통해 분석되었다. Cpne7-DP는 상아모세포로의 분화를 촉진시키고 세관 상아질의 재생을 도모한다. 또한 CPNE7 단백질과 Cpne7-DP가 다양한 깊이의 상아질 손상 모델에서 상아질의 생리적인 세관 구조를 유지하는 새로운 경조직 재생을 유도하는 것을 관찰하였다.

Cpne7-DP의 기능에 대한 종합적인 분석을 통해 생체활성 치료 물질로서의 Cpne7-DP의 가능성을 확인한 본 논문의 결과는 Cpne7-DP가 생리적인 세관 상아질의 재생과 관주공간의 폐쇄를 촉진하며, 이는 상아질 손상 및 과민증을 유발하는 구강 질환의 치료에 적용될 수 있음을 시사한다.

주요어 : 상아모세포, 상아질 형성, 바이오소재, 경조직, 조직 발생

학 번 : 2014-23078